e-J. Surf. Sci. Nanotech. Vol. 7 (2009) 831-835 Regular Paper

Metal-Interface Second Harmonic Generation from Pt/Cu Bimetallic Nanowire Arrays on NaCl(110) Faceted Templates

Nguyen Anh Tuan and Goro Mizutani*
School of Materials Science,
Japan Advanced Institute of Science and Technology,
1-1 Asahidai, Nomi, Ishikawa 923-1292, Japan
(Received 20 June 2009; Accepted 29 July 2009; Published 5 September 2009)

We have obtained the azimuthal angle dependence of the second harmonic (SH) intensity from bimetallic Pt/Cu and Pt/SiO/Cu nanowire arrays. The arrays were fabricated by shadow deposition on NaCl(110) faceted templates. The SH intensity from the Pt/Cu nanowire array measured in S_{in}/S_{out} polarization combination were 4.7 times larger than that from the Pt/SiO/Cu nanowire array at the fundamental photon energy of 2.33 eV. Phenomenological analysis of the intensity patterns and numerical calculation of the local fields have shown that the inversion symmetry broken at the metal-metal interface is responsible for the enhanced SH generation from the Pt/Cu bimetallic nanowire arrays. [DOI: 10.1380/ejssnt.2009.831]

Keywords: Metal-Interface; Second harmonic generation; Bimetallic nanowire; finite-difference time-domain method; Copper; Platinum; NaCl(110)

I. INTRODUCTION

Unique properties of nanometer-scale materials due to the spatial confinement of their electrons have led to novel applications, such as the Coulomb blockade to single electron transistors (SET) and superparamagnetism to giant magnetoresistive (GMR) sensors. Recently, metallic nanowire structures have generated considerable interest due to their strong anisotropy in the electron confinement, electrical conductivity and resulting optical properties. Their potential applications to nonlinear optics [1], surface enhanced Raman scattering [2], and plasmonics [3] have been proposed.

Metallic nanowire arrays prepared by a shadow deposition method are particularly interesting because of the large areas of periodically aligned nanowires sufficient for optical measurements as well as applications. Second harmonic generation (SHG) has been used as one of the fine tools to characterize the electronic response of the nanowires on the surface and interface of such materials [4]. Along with linear optical measurements [5], the nonlinear optical investigations on Au [1], Pt [6] and Cu [7] nanowire arrays showed the anisotropic nature of these structures. The suppression of SH intensity due to the electric depolarization field was observed for Au nanowires [8] but was not for Pt nanowires [6]. Besides, the SH response caused by a resonant coupling between the fundamental field and the surface plasmon was observed in Cu nanowires [9]. With this accumulation of knowledge of nonlinear optical properties of nanowires of important metal species, we should now turn to new nanoscopic materials.

In order to develop new second-order nonlinear optical materials with more artificial anisotropy, we adopt two wire materials and have coupled them in nanowire structures. In the array of the bimetallic nanowire structure, the nonlinearity at the interface of the two different-metal nanowires is expected to induce a macroscopic nonlinearity. However, this kind of attempt has never been done, so far as we know.

In this work, we measure the azimuthal angle dependence of SHG from Pt/Cu bimetallic nanowire arrays prepared by a shadow deposition method [10]. Platinum and copper were chosen because their work function difference is significant among important metals. We have found enhancement of SH intensity from the Pt/Cu bimetallic nanowire arrays as compared to that from a control sample, Pt/SiO/Cu nanowires. Phenomenological analysis and finite-difference time-domain (FDTD) simulation show that a major contribution to the enhanced SHG from the Pt/Cu nanowire arrays comes from the asymmetric cross-interfacial currents.

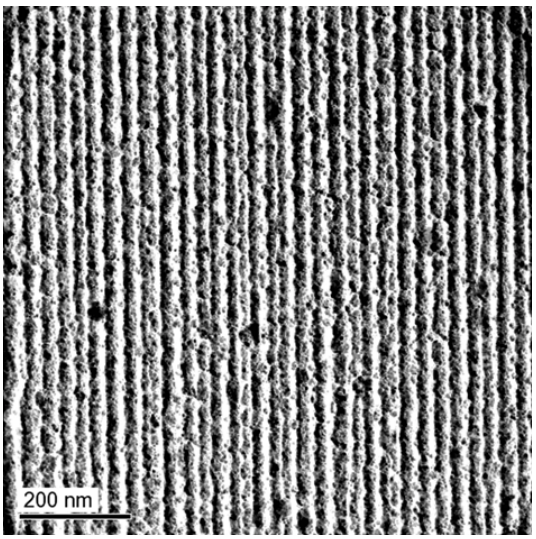

FIG. 1: The Pt/Cu nanowire array deposited on the NaCl(110) faceted template, as observed in bright field TEM images. The Pt/Cu nanowires, seen in dark contrast, run along the [001] azimuth of the NaCl(110) substrate. The darker stripe in each nanowire is the overlap region of the platinum and the copper.

*Corresponding author: mizutani@jaist.ac.jp

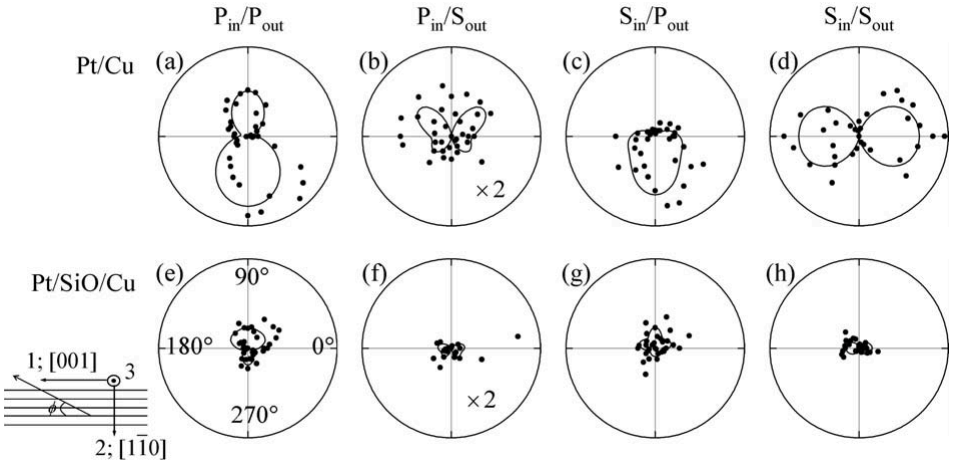

FIG. 2: SH intensity from the Pt/Cu bimetallic nanowires (a-d) and Pt/SiO/Cu sandwich nanowires (e-h) on the NaCl(110) faceted templates for $2\hbar\omega$=4.66 eV as a function of the sample rotation angle ϕ for the four different input/output polarization combinations indicated at the top. The intensity scales are the same except that those in P_{in}/S_{out} polarization combination have been magnified 2 times. The rotation angle ϕ is the angle between the incident plane and the [001] direction (parallel to the nanowire axis) of the NaCl(110) template as shown in the inset. At the sample rotation angle ϕ=270° the incident fundamental beam is defined to travel in the same direction as the Pt or Cu atomic beam during the deposition.

II. EXPERIMENTAL

Sample preparation was performed in UHV (1.3×10^{-7} Pa). The NaCl(110) substrate was etched by water for 10 seconds before being loaded into the UHV chamber. Then it was annealed at 400°C for 1 hour to produce a clean faceted surface. The facet formation was monitored by reflection high energy electron diffraction (RHEED). Amorphous SiO was deposited as a passivation layer with thickness of 10 nm on the faceted NaCl(110). Then Cu and Pt were successively deposited with an incident angle of 65° from the template normal. The nominal deposition thicknesses of Cu and Pt were 9 nm and 7 nm, respectively. The interval between these two depositions was sufficient for cooling down the NaCl substrate to room temperature. Finally, another 10-nm-thick SiO passivation layer was deposited on top of the nanowire array.

In the sample preparation for transmission electron microscopy (TEM) observation with a Hitachi HF-2000 transmission electron microscope, the Pt/Cu wire array, sandwiched by the SiO layers, was floated off the NaCl substrate in water. Figure 1 shows a bright field TEM image of the nanowire array. The Pt/Cu bimetallic nanowires, seen in dark contrast, run along the [001] direction of the NaCl(110) substrate. The average width and period of the bimetallic nanowires were 20 nm and 40 nm, respectively. No other phase than polycrystalline Pt and Cu was detected by the electron diffraction analysis of the Pt/Cu bimetallic nanowires.

Very dark areas representing the double layers of platinum on copper are seen to form long bimetallic nanowires, although islands are seen in the surrounding area. These island structures have been reported to give isotropic contribution to SH intensity as a function of the azimuthal angle around the surface normal [1].

Another nanowire array with a 5-nm-thick SiO layer sandwiched between Pt and Cu nanowires was fabricated as a control sample. In this Pt/SiO/Cu nanowire array, the SiO layer secured that no metal-metal interface was formed between Pt and Cu. No significant difference in microstructure between this sample and the Pt/Cu bimetallic nanowire array was observed by TEM.

For the SHG measurements, we used a frequency doubled output of a mode-locked cavity-damped Nd:YAG laser with the photon energy of 2.33 eV. We did not use the fundamental output of the Nd:YAG laser at 1.17 eV because the Pt nanowires were easily damaged due to its strong optical absorption at this photon energy [11]. The SH intensity as a function of the azimuthal angle around the surface normal was measured in the reflection direction with the incident angle of 45°. The SH light was selected by a monochromator and detected by a photomultiplier tube (PMT). The signal from the PMT was integrated by a boxcar integrator (Stanford Research Systems, SR250). The measurements for the two types of samples were carried out under the same optical arrangement and with normalized laser power.

III. RESULTS AND DISCUSSIONS

The dots in Fig. 2 show the SH intensities from the Pt/Cu nanowires (a-d) and the Pt/SiO/Cu nanowires (e-h) on the NaCl(110) templates as a function of the azimuthal angle. The azimuthal angle ϕ is defined as the angle between the incident plane and the nanowire axis, as depicted in the inset of Fig. 2. The four patterns for each sample correspond to four different polarization combinations of the incident/SH light displayed at the top of Fig. 2. For all the polarization combinations, the SH intensity patterns are quite anisotropic.

The azimuthal angle dependences were measured over a large area of the nanowire arrays when rotating the samples around their surface normal. Consequently, the obtained SH intensity patterns are typical of the collective response of many nanowires in the arrays. We have fab-

ricated another array of Pt/Cu bimetallic nanowires and the SH intensity patterns obtained from it are consistent with those in Fig. 2 from a point of view of the overall pattern shapes.

On the other hand, we see rather large intensity fluctuation in all the SH intensity patterns. One fluctuation source of the SH intensity can be the island structures existing around the nanowires as seen in the TEM images. The other source came from the less mirrorlike surface of the NaCl templates due to the water etching process of the sample preparation. This water etching is necessary for forming well-ordered microscopic facets on the substrate, but it deteriorates the macroscopic optical flatness of the sample surface. Since the measured point on the substrate moves as the sample is rotated, the surface roughness irregularly modifies the signal intensity. These fluctuations could not be removed even when the accumulation time was increased.

We analyzed the measured SH intensity patterns by using a phenomenological model in nonlinear optics [12]. In this model, the internal fundamental field strength in the nanowire layer was calculated by Maxwell equations under appropriate boundary conditions. This layer was treated as a homogeneous medium. Next, the nonlinear polarization $P_i(2\omega) = \varepsilon_0 \chi^{(2)}_{ijk}$: $E_i E_j$ was calculated. Here $\chi^{(2)}_{ijk}$ is a third rank tensor of the second-order susceptibility. Then the reflected SH intensity was obtained by the electromagnetic wave equation and Maxwell's boundary conditions. Ten independent nonlinear susceptibility elements: $\chi^{(2)}_{113}, \chi^{(2)}_{223}, \chi^{(2)}_{311}, \chi^{(2)}_{322}, \chi^{(2)}_{333}, \chi^{(2)}_{211}, \chi^{(2)}_{222}, \chi^{(2)}_{233}, \chi^{(2)}_{121}$ and $\chi^{(2)}_{323}$ of Cs symmetry [13] are allowed for the Pt/Cu and Pt/SiO/Cu nanowire structures. The suffixes 1, 2 and 3 represent the [001], [1$\bar{1}$0], and [110] directions on the NaCl(110) template, respectively, as indicated in the inset of Fig. 2.

Figure 3 shows the calculated SH intensity patterns obtained by setting each nonlinear susceptibility element to a certain finite value and all the other elements as zero. The theoretical SH intensity is a linear combination of the patterns in Fig. 3 in the complex plane with the multiplication factors of $\chi^{(2)}_{ijk}$'s.

We fitted the theoretical SH intensity patterns to the experimental data by varying the values of the $\chi^{(2)}_{ijk}$ elements in the complex plane, using a least-squares fitting algorithm. The results are shown in Fig. 2 in solid curves. The SH intensity patterns for S_{in}/S_{out} polarization combination in Figs. 2(d) and (h) are dominated by the contribution of $\chi^{(2)}_{222}$ element, as we can easily judge it from Fig. 3. The ratio of $|\chi^{(2)}_{222}|$ of the Pt/Cu nanowire array to that of the Pt/SiO/Cu nanowire array is 2.2:1. This ratio gives a factor of 4.7 of the enhanced SH intensity from the Pt/Cu nanowires as observed experimentally in the S_{in}/S_{out} configuration [Fig. 2 (d, h)].

As seen in Fig. 3, the observed SH intensities for the S_{in}/P_{out} combination at the azimuthal angles of 0° and 180° are contributed by the $\chi^{(2)}_{322}$ element only. The SH intensities from the Pt/Cu nanowires in the S_{in}/P_{out} configuration [Fig. 2(c)] at the azimuthal angles of 0° and 180° were 1.3 times larger than that from Pt/SiO/Cu nanowires [Fig. 2(g)]. Accordingly, the calculated value of $|\chi^{(2)}_{322}|$ of Pt/Cu nanowires was 1.13 times larger than that of Pt/SiO/Cu nanowires.

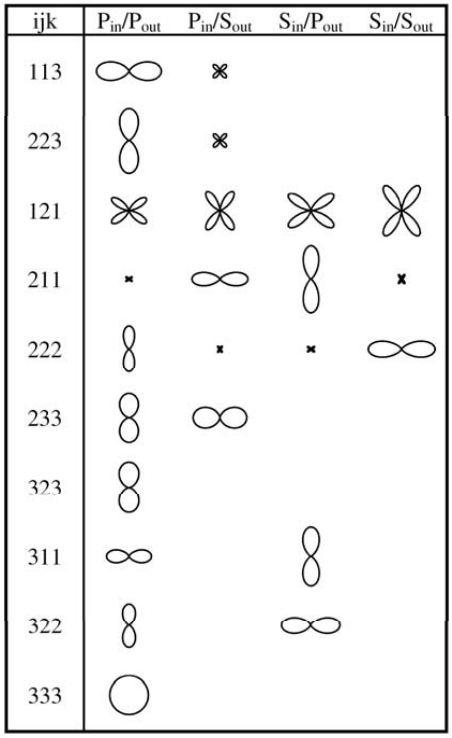

FIG. 3: SH intensity patterns obtained by a theoretical calculation when one of the nonlinear susceptibility elements $\chi^{(2)}_{ijk}$ is set equal to a certain common value and all of the other elements are set equal to zero. The intensities in the same row are in common units. Patterns are not shown when the calculated intensity is negligible.

The observed SH intensity patterns for the polarization combinations other than S_{in}/S_{out} were contributed by more than one susceptibility element. In particular, both $\chi^{(2)}_{211}$ and $\chi^{(2)}_{311}$ elements contribute to the SHG at the azimuthal angles of 90° and 270° for the S_{in}/P_{out} combination as it is seen in Fig. 3. The obtained phase angles in the complex plane between the $\chi^{(2)}_{211}$ and $\chi^{(2)}_{311}$ elements were 0.82π and 0.32π for Pt/Cu nanowires and Pt/SiO/Cu nanowires, respectively. Thus the interference between the $\chi^{(2)}_{211}$ and $\chi^{(2)}_{311}$ elements is negative in the Pt/Cu nanowires and is positive in the Pt/SiO/Cu nanowires. For this reason, for the S_{in}/P_{out} polarization combination, the SH intensity from the Pt/Cu nanowires is strong around the azimuthal angle of ϕ=270° [Fig. 2(c)], whereas that from the Pt/SiO/Cu nanowires is strong around ϕ=90° [Fig. 2(g)].

It has been generally shown that the local enhancement of the fundamental electric field in metallic nanostructures can enhance the SH response [14]. To check this possibility in our case, we have calculated the distribution of the local electric field in the Pt/Cu nanowire array using the finite-difference time-domain (FDTD) method.

Assuming that the length of the metal nanowires was infinite, the simulations were performed in a 2-D plane perpendicular to the wire axes with the elliptic or rectangular cross-sectional shapes. The width and the thickness of the simulated nanowires were set as the same as the fabrication parameters. The long axes of the cross-sectional

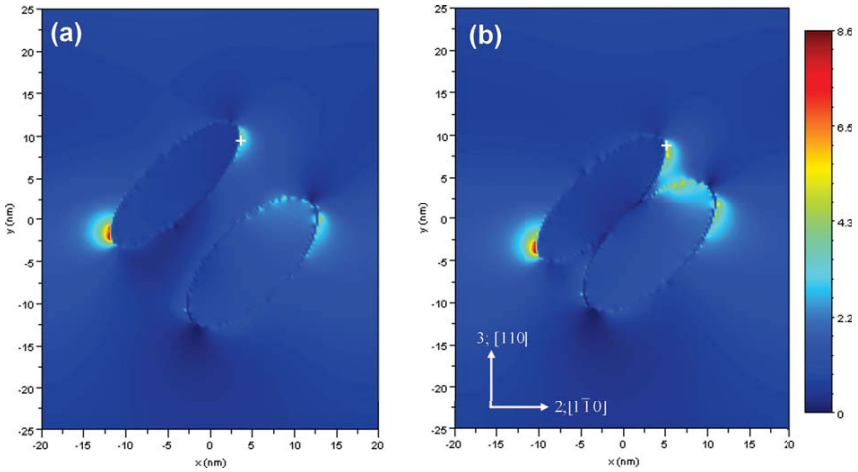

FIG. 4: 2-polarized electric field intensities around the Pt/SiO/Cu structure (a) and the Pt/Cu structure (b) of nanowires of the elliptic cross-sectional shape calculated by the FDTD method. The Pt nanowire is above the Cu nanowire in the both structures. The intensity scale is shown on the right. The maximum intensities in the upper right hand corners are marked by "+".

shapes of the nanowires were tilted by 45° because they had been fabricated on the (010) faces of the NaCl(110) faceted template. The simulation areas were filled with a medium with the dielectric constant of SiO. Material parameters of Pt and Cu were defined according to the experimental dielectric functions [11]. A plane-wave source of wavelength 532 nm with the electric field polarized in the direction 2 (2-polarized) was assumed to simulate the incident fundamental light in S_{in} polarization at the azimuthal angle of 0° and 180°. The periodic boundary condition was used to simulate the array structure. After the calculation converged, the intensity distributions of the 2-polarized electric fields were obtained for the four combinations of the structures of the Pt/SiO/Cu and the Pt/Cu nanowires with the elliptic and rectangular cross-sectional shapes.

Figure 4 shows the 2-polarized electric field intensities calculated by the FDTD method for the Pt/SiO/Cu structure (a) and the Pt/Cu structure (b) with the elliptic cross-sectional shapes. The normalized field intensities are indicated by the color-scale bar. The result of the simulations of the rectangular nanowires (not shown here) gave no significant difference in the local electric field between the Pt/Cu and Pt/SiO/Cu structures.

As seen in Fig. 4, the field intensity around the nanowire in the upper right hand corner is enhanced when nanowires contact each other in the Pt/Cu structure [Fig. 4(b)]. The maximum electric field intensity in this area, marked by "+" in Fig. 4, increases 1.3 times between these two structures. This 2-polarized local field enhancement leads to 1.7 times enhancement of SH intensities induced by the $\chi^{(2)}_{222}$ and $\chi^{(2)}_{322}$ elements according to a straightforward application of the quadratic SHG process. However, we observed enhancement factors of 4.7 and 1.3 for the SH intensity due to the $\chi^{(2)}_{222}$ and $\chi^{(2)}_{322}$ elements in S_{in}/S_{out} and S_{in}/P_{out} polarization combinations, respectively. Hence the local electric field enhancement was not dominant in the enhanced SHG from the Pt/Cu bimetallic nanowires. The enhancement of the SH intensity induced by the $\chi^{(2)}_{222}$ element is dominated by the symmetry breaking in the direction 2 in the Pt/Cu nanowire array. To the first order approximation the Pt and Cu nanowires are considered to have symmetric cross section, and the symmetry breaking occurs at the Pt/Cu interface.

Rudnick and Stern have successfully described the nature of the SH response in the surface region of a jellium-metal [15]. They introduced a mechanism for producing the normal surface current by taking into account the inversion symmetry breaking at the metal surface. The nonlinearity was originated from the asymmetric movement of electrons at the surface.

The mechanism proposed by Rudnick and Stern can be applied to explain qualitatively the enhancement of the SH intensity induced by the $\chi^{(2)}_{222}$ element in the Pt/Cu bimetallic nanowires. The direction 2 is perpendicular to the nanowires' axes, as defined in Fig. 2. In the interface region between the Pt and Cu nanowires, the difference of the work functions between Pt and Cu creates an asymmetric potential for the electron movement in the direction normal to the interface. Due to this asymmetric potential, the electrons flowing from Pt to Cu are freer to move than when they flow from Cu to Pt. This condition is suggested to cause the nonlinearity in the direction 2.

The measurement of the wavelength dependence of the SH intensity from the Pt/Cu bimetallic nanowires is under way to maximize the enhancement effect and to get an insight into the mechanism of the nonlinearity. Dependence on the combination of the metals should also be investigated.

IV. CONCLUSIONS

We have fabricated Pt/Cu bimetallic nanowire arrays on the NaCl(110) faceted templates by a shadow deposition method. The enhancement was observed in the azimuthal angle dependence of the SH intensity from the Pt/Cu nanowire arrays for the four polarization combinations. From the phenomenological analysis and FDTD

calculations the enhanced SHG from the Pt/Cu nanowires in the S_{in}/S_{out} configuration has been judged to originate from the increase of the $\chi^{(2)}_{222}$ in the bimetallic nanowire structure. We also found that the interference between $\chi^{(2)}_{211}$ and $\chi^{(2)}_{311}$ elements of Pt/Cu nanowires was different from that of Pt/SiO/Cu nanowires.

Acknowledgments

The authors would like to thank Dr. H. Sano and Dr. A. Sugawara for valuable discussion and advice. We thank K. Higashimine for his support in our TEM observation.

[1] T. Kitahara, A. Sugawara, H. Sano, and G. Mizutani, Appl. Surf. Sci. **219**, 271 (2003).
[2] Z.-Q. Tian, B. Ren, and D.-Y. Wu, J. Phys. Chem. B **106**, 9463 (2002).
[3] W. L. Barnes, A. Dereux, and T. W. Ebbesen, Nature **424**, 824 (2003).
[4] R. W. Boyd, *Nonlinear Optics* (Academic Press, San Diego, 2003).
[5] G. Schider, J. R. Krenn, W. Gotschy, B. Lamprecht, H. Ditlbacher, A. Leitner, and F. R. Aussenegg, J. Appl. Phys. **90**, 3825 (2001).
[6] N. Hayashi, K. Aratake, R Okushio, T. Iwai, A. Sugawara, H. Sano, and G. Mizutani, Appl. Surf. Sci. **253**, 8933 (2007).
[7] K. Locharoenrat, H. Sano, and G. Mizutani, J. Lumin. **128**, 824 (2008).
[8] T. Kitahara, A. Sugawara, H. Sano, and G. Mizutani, J. Appl. Phys. **95**, 5002 (2004).
[9] K. Locharoenrat, H. Sano, and G. Mizutani, J. Phys.: Conf. Ser. **100**, 052050 (2008).
[10] A. Sugawara, G.G. Hembree, and M.R. Scheinfein, J. Appl. Phys. **82**, 5662 (1997).
[11] E. D. Palik, *Handbook of Optical Constants of Solids* (Academic Press, San Diego, 1985).
[12] M. Omote, H. Kitaoka, E. Kobayashi, O. Suzuki, K. Aratake, H. Sano, G. Mizutani, W. Wolf, and R. Podloucky, J. Phys.: Condens. Matter **17**, S175 (2005).
[13] P.-F. Brevet, *Surface Second Harmonic Generation*, (Press Polytechniques et Universitaires Romandes, Lausanne, 1997).
[14] A. Lesuffleur, L. K. S. Kumar, and R. Gordon, Appl. Phys. Lett. **88**, 261104 (2006).
[15] J. Rudnick and E. A. Stern, Phys. Rev. B **4**, 4274 (1971).